International Journal of Advanced Science and Research
www.allsciencejournal.com
ISSN: 2455-4227
Received: 16-02-2026, Accepted: 19-03-2026, Published: 03-04-2026
Volume 11, Issue 2, 2026, Page No. 7-15

Enhanced petroleum hydrocarbon removal via integrated nano-phytoremediation: Synergistic coupling of water hyacinth and zero-valent iron nanoparticles

Adeyemi, Oyeyemi[1, 2]*, Akpomedaye Efe Cletus[1]
[1, 2] Department of Environmental Management and Toxicology, Federal University of Petroleum Resources, Effurun, Delta State, Nigeria
[2] Department of Biochemistry, Federal University of Petroleum Resources, Effurun, Delta State, Nigeria
Corresponding Author: Adeyemi, Oyeyemi

Abstract
Petroleum hydrocarbon contamination in aquatic systems poses persistent ecological and toxicological risks, necessitating efficient and sustainable remediation strategies. This study assessed the efficacy of an integrated nano-phytoremediation system combining *Eichhornia crassipes* and nanoscale zero-valent iron (nZVI) for removing crude petroleum oil from contaminated water. Experimental setups with 1000 ppm CPO included control, phytoremediation-only, nZVI-only, and hybrid treatments monitored over 28 days. Results revealed a clear hierarchy in total petroleum hydrocarbon removal efficiency, with hybrid systems achieving significantly greater reductions than standalone treatments. By week 4, TPH levels in the highest-dose hybrid system declined from an initial 5.10 ± 0.22 mg/L to 1.28 ± 0.10 mg/L, compared to 2.96 ± 0.18 mg/L for phytoremediation alone and 2.21 ± 0.15 mg/L for nZVI-only. This superior performance stems from synergistic mechanisms, including adsorption, reductive transformation, rhizodegradation, and biomass sequestration. Plant physiological responses further supported remediation success, with SPAD chlorophyll indices recovering significantly in nano-assisted treatments—indicating reduced oxidative stress and enhanced photosynthetic stability. Notably, hydrocarbon accumulation in plant tissues rose up to 2.3-fold in hybrid systems, underscoring biomass partitioning as a complementary removal pathway. Overall, the integrated nano-phytoremediation approach offers a robust, scalable, and mechanistically synergistic strategy for petroleum hydrocarbon remediation in aquatic environments, with broad implications for sustainable water treatment technologies.

Keywords: Nano-phytoremediation, petroleum hydrocarbons, Eichhornia Crassipes, zero-valent iron nanoparticles, aquatic bioremediation

Introduction

Petroleum hydrocarbon contamination of aquatic environments remains a critical global environmental challenge due to its persistence, toxicity, and complex multiphase behavior in water systems(Panneerselvan *et al*., 2018) [41]. Crude petroleum oil introduces a mixture of aliphatic and aromatic hydrocarbons alongside associated trace metals (Overton *et al*., 2016) [40], which collectively disrupt aquatic ecosystems, impair water quality, and induce oxidative stress in exposed biota (Alzahrani & Rajendran, 2019) [5]. The environmental fate of these contaminants is governed by processes such as volatilization, dissolution, adsorption, and microbial degradation (Truskewycz *et al*., 2019) [55]. However, natural attenuation alone is often insufficient for effective remediation in heavily contaminated systems (Raju & Scalvenzi, 2018) [43]. Consequently, there is a growing need for innovative remediation strategies that integrate physicochemical and biological processes to enhance contaminant removal efficiency.

Phytoremediation has emerged as a sustainable and cost-effective approach for mitigating hydrocarbon pollution in aquatic systems (Mohammed & M-Ridha, 2019; Sharma *et al*., 2024) [37, 47]. Aquatic macrophytes such as *Eichhornia crassipes* exhibit remarkable adaptive plasticity, rapid biomass production, and extensive root systems that facilitate contaminant uptake, adsorption, and rhizosphere-mediated degradation. These traits enable partial recovery of water quality and plant physiological functions under contaminant stress (Bais *et al*., 2016 [10]; Monroy-Licht *et al*., 2024). Nevertheless, phytoremediation alone is limited by slow remediation kinetics, incomplete degradation of recalcitrant hydrocarbon fractions, and potential accumulation of contaminants in plant tissues, which can restrict overall efficiency (Azubuike *et al*., 2016) [9].

Recent advances in nanotechnology have introduced nanoscale zero-valent iron (nZVI) as a highly reactive material for environmental remediation(Garg *et al*., 2024; Liu *et al*., 2024) [20, 34]. nZVI offers strong reductive capacity, high surface area, and rapid adsorption kinetics, enabling effective transformation and immobilization of petroleum hydrocarbons and associated contaminants(Kane *et al*., 2026; Liu *et al*., 2024) [28, 34]. In aqueous systems, nZVI facilitates hydrocarbon removal through adsorption and catalytic reduction pathways, thereby accelerating remediation processes compared to biological systems alone(Albarano *et al*., 2022; Kane *et al*., 2026) [2, 28]. Additionally, the transformation of nZVI into iron oxides may enhance micronutrient availability, indirectly supporting plant physiological recovery under stress conditions(Razzaq *et al*., 2022; Yoon *et al*., 2019) [45, 57].

The integration of phytoremediation and nanotechnology has gained attention as a hybrid approach that overcomes the limitations of standalone techniques (Gomes, 2025; Wentzell, 2025) [23, 56]. In these systems, plants provide ecological stabilization, continuous uptake, and rhizosphere enhancement (Asare *et al*., 2023; Rao *et al*., 2010) [8, 44], while nanoparticles deliver rapid contaminant reduction and

adsorption (Gomes, 2025) [23]. This synergistic interaction creates a multi-mechanistic remediation pathway involving adsorption, catalytic transformation, microbial stimulation, and biomass sequestration (Gomes, 2025) [23]. Evidence indicates that hybrid nano-phytoremediation systems achieve superior hydrocarbon removal compared to individual treatments, with efficiency increasing in a dose-dependent manner as nanoparticle concentration rises(Steliga *et al*., 2026; Ting *et al*., 2021) [52, 53].

Despite these advances, integrated evaluations of hydrocarbon removal dynamics, plant physiological responses, and contaminant partitioning in nano-assisted phytoremediation systems remain limited(El-Ramady *et al*., 2020; Liu *et al*., 2025) [18, 35]. In particular, the contribution of biomass accumulation alongside aqueous-phase depletion is not fully elucidated, and the mechanistic interplay between biological uptake and nanoparticle-mediated catalysis requires further clarification(El-Ramady *et al*., 2020; Liu *et al*., 2025) [18, 35]. Hydrocarbon accumulation in plant tissues observed in contaminated systems underscores the importance of understanding bioaccumulation dynamics within the overall remediation framework (Aliyeva, 2024; Kassenga, 2017) [3, 29].

Therefore, this study investigates the efficacy of a hybrid nano-phytoremediation system combining *Eichhornia crassipes* and nanoscale zero-valent iron for treating crude petroleum oil-contaminated water. The study aims to elucidate the synergistic mechanisms governing hydrocarbon removal, evaluate the influence of nanoparticle dosage on remediation efficiency, and assess the role of plant physiological responses and bioaccumulation in shaping overall system performance. This integrated approach provides critical insights into developing scalable and sustainable remediation technologies for petroleum-contaminated aquatic environments.

Materials and Methods

Experimental Design

A controlled laboratory study evaluated the efficiency of an integrated nano-phytoremediation system for petroleum hydrocarbon removal from contaminated water. Treatments comprised four categories—control (contaminated water without remediation), phytoremediation with *Eichhornia crassipes*, nanoscale zero-valent iron (nZVI) treatment, and hybrid nano-phytoremediation—each conducted in triplicate over 28 days.

Synthetic contaminated water was prepared by spiking tap water with Bonny Light crude oil to a final concentration of 1000 ppm.

Preparation and Application of nZVI

nZVI was synthesized using the method described by (Kane *et al*., 2026) [28] and applied at 0.1, 0.2, and 0.4 mg/kg. These concentrations enabled evaluation of dose-dependent remediation efficiency while minimizing phytotoxicity. nZVI promotes hydrocarbon removal through adsorption and reductive transformation, driven by its high surface reactivity(Ji *et al*., 2023; Kane *et al*., 2026) [28].

Plant Material and Phytoremediation Setup

Healthy *Eichhornia crassipes* plants were collected, acclimatized, and introduced into treatment systems. The species' rapid growth, extensive root architecture, and adaptive plasticity facilitate contaminant uptake and rhizosphere-mediated degradation (Monroy-Licht *et al*., 2024; Shingadgaon, 2018) [48].

Hybrid systems combined plants with nZVI to harness synergistic mechanisms, including adsorption, catalytic transformation and biomass sequestration (Gomes, 2025) [23].

Determination of Total Petroleum Hydrocarbons

Total petroleum hydrocarbons in water and plant tissues were quantified via gas chromatography–mass spectrometry (GC–MS). Samples underwent n-hexane liquid–liquid extraction, concentration, and GC–MS injection. Hydrocarbon fractions were identified and quantified using retention times and spectral matching against standard libraries.

Elemental Analysis

Elemental composition of water samples was determined by inductively coupled plasma optical emission spectrometry following acid digestion. Calibration with certified multi-element standards enabled quantification of metals such as Ba, Zn, Pb, Ca, and Mg, providing baseline contamination levels and assessing remediation-induced metal removal.

Physicochemical Characterisation of Crude Oil

Physicochemical properties of the crude oil were characterized prior to experimentation using standard procedures. Density and specific gravity were measured via hydrometer, viscosity with a viscometer at controlled temperature, and pH using a calibrated pH meter. Total dissolved solids and electrical conductivity were also evaluated as applicable.

Hydrocarbon composition was analyzed by GC–MS, with associated trace metals quantified by ICP-OES. This comprehensive profiling established an accurate baseline for the contaminant matrix and remediation dynamics.

Plant Physiological Assessment

Chlorophyll content (SPAD index) was used to assess plant physiological status. Leaf relative water content was determined by measuring fresh and turgid weights, providing insights into plant water status and photosynthetic efficiency (Trepanier *et al*., 2023) [54].

Mechanistic Considerations

Hydrocarbon removal integrated physicochemical and biological processes (Caumette *et al*., 2012) [16], including nZVI adsorption, reductive transformation (Albarano *et al*., 2022) [2], and plant uptake (Banerjee *et al*., 2016) [11]. Hybrid systems synergistically boosted efficiency via concurrent pathway activation (Broholm *et al*., 2015; Sohrabnezhad *et al*., 2026) [15, 49].

Statistical Analysis

Data are reported as mean ± standard error of mean from triplicates. One-way ANOVA with post-hoc tests assessed significance ($p < 0.05$).

Results and Discussion

The initial characterization of the experimental system, as presented in Tables 1–3, establishes the physicochemical and toxicological baseline necessary for interpreting remediation performance. The elemental composition of the experimental tap water confirms a chemically stable and regulation-compliant aqueous matrix, with all measured

parameters within WHO and NESREA permissible limits—for instance, As at 0.005 ± 0.002 mg/L (<0.01 mg/L WHO), Cd at 0.001 ± 0.001 mg/L (<0.01 mg/L NESREA), Pb at 0.003 ± 0.002 mg/L (<0.01 mg/L WHO), Cr at 0.01 ± 0.01 mg/L (=0.05 mg/L WHO/NESREA), Ni at 0.005 ± 0.003 mg/L (<0.07 mg/L WHO), Se at 0.005 ± 0.002 mg/L (<0.04 mg/L WHO), and Tl at 0.0005 ± 0.0003 mg/L (<0.002 mg/L WHO). These notably low concentrations of toxic trace elements indicate that the system was not predisposed to metal-induced oxidative stress prior to contamination, as background metal loads can independently trigger reactive oxygen species formation via redox cycling or Fenton-like reactions, thereby confounding remediation outcomes(Kaur *et al*., 2019) [30]. The presence of essential ions at moderate concentrations—e.g., Ca (12.50 ± 0.60 mg/L), Mg (18.50 ± 0.90 mg/L), and Zn (1.20 ± 0.10 mg/L)—further supports ionic balance and physiological stability of *Eichhornia crassipes*, ensuring that plant performance during remediation is not limited by nutrient deficiency or osmotic stress.

The physicochemical properties of the crude petroleum oil reveal a contaminant matrix characterised by high environmental persistence and limited natural attenuation. The high kinematic viscosity (106.49 ± 1.23 $mm^2 s^{-1}$ at 40 °C; 8.918 ± 0.10 $mm^2 s^{-1}$ at 100 °C) and specific gravity (0.9582 ± 0.0111 at 15 °C) indicate restricted dispersion(Olugbenga *et al*., 2020) [39], enhanced adhesion to surfaces, prolonged residence time in aquatic systems, and reduced bioavailability for microbial or plant-mediated degradation(Khodja *et al*., 2010) [32]. The low viscosity index (23.10 ± 0.27) further suggests strong temperature dependence(Souas *et al*., 2025) [51], implying increased rigidity under typical environmental conditions (e.g., pour point of −18 ± 0.21 °C and cloud point of 24 ± 0.28 °C), which exacerbates hydrocarbon immobility(Soliman, 2019) [50]. Additionally, the moderate sulphur content (0.4388 ± 0.0051% w/w) introduces the potential for secondary acidification during any microbial degradation, altering metal solubility, pH, and redox equilibrium(Basafa & Hawboldt, 2018, 2020) [12, 13]. These physicochemical constraints empirically explain the persistence of hydrocarbons in untreated systems (as later confirmed in Table 4) and underscore the necessity for active remediation strategies.

The elemental composition of the crude oil further demonstrates that the contaminant is not solely hydrocarbon-based but constitutes a complex multi-metal pollutant system. Elevated concentrations of transition and heavy metals—including Cr (6757.53 ± 195.07 mg/kg), Cu (4264.33 ± 123.07 mg/kg), V (2019[19].42 ± 58.29 mg/kg), Pb (192.87 ± 5.56 mg/kg), and as (25.90 ± 0.75 mg/kg)—confirm substantial metal enrichment within the crude oil matrix. Transition metals such as Cr and V catalyse ROS generation through redox cycling, while Cu participates in Fenton-like reactions, intensifying oxidative stress; Pb and As introduce additional toxicity through enzyme inhibition and binding to thiol (-SH)-containing biomolecules, as As inactivates over 200 enzymes and heavy metals displace essential ions in metalloproteins (Engwa *et al*., 2019; Kaur *et al*., 2019) [19, 30].

Importantly, the coexistence of hydrocarbons and metals establishes a synergistic toxicity framework, where hydrocarbons disrupt membrane integrity to facilitate intracellular metal penetration, while metals amplify hydrocarbon-induced oxidative damage through catalytic ROS production (Gauthier *et al*., 2014) [21]. This dual-mode stress—evidenced by the metal burdens in **Table 3**—significantly enhances the ecological risk of petroleum contamination compared with single-contaminant systems(Zhang *et al*., 2023) [58], creating a chemically complex environment that demands multifaceted remediation.

Collectively, Tables 1–3 define three critical baseline conditions: the experimental aqueous system was chemically stable and free from confounding contamination; the crude oil exhibited high viscosity, persistence, and resistance to natural attenuation; and the contaminant matrix carried a substantial burden of redox-active metals capable of intensifying oxidative stress. These foundational characteristics provide the mechanistic basis for understanding the superior treatment-dependent hydrocarbon removal, elemental redistribution, and bioaccumulation patterns observed in subsequent sections (e.g., Table 4).

Table 1: Elemental Analysis of Experimental Tapwater Sample

Element	Tap Water (mg/L, Mean ± SD)	WHO Guideline (mg/L)	NESREA Guideline (mg/L)	Compliance
Ag	0.03 ± 0.01	0.10	–	Acceptable
Al	0.08 ± 0.02	0.20	0.50	Acceptable
As	0.005 ± 0.002	0.01	0.05	Acceptable
Ba	0.12 ± 0.03	0.70	0.10	Acceptable*
Be	0.00 ± 0.00	–	–	Acceptable
Ca	12.50 ± 0.60	–	–	Acceptable
Cd	0.001 ± 0.001	0.00	0.01	Acceptable
Co	0.00 ± 0.00	–	–	Acceptable
Cr	0.01 ± 0.01	0.05	0.05	Acceptable
Cu	0.20 ± 0.05	2.00	1.00	Acceptable
Fe	0.10 ± 0.03	0.30	0.30	Acceptable
K	2.80 ± 0.20	–	–	Acceptable
Mg	18.50 ± 0.90	50.00	–	Acceptable
Mn	0.03 ± 0.01	0.10	0.20	Acceptable
Na	8.20 ± 0.50	–	–	Acceptable
Ni	0.005 ± 0.003	0.07	0.02	Acceptable
Pb	0.003 ± 0.002	0.01	0.05	Acceptable
Se	0.005 ± 0.002	0.04	0.01	Acceptable
Th	0.00 ± 0.00	–	–	Acceptable
Tl	0.0005 ± 0.0003	0.002	–	Acceptable
U	0.010 ± 0.004	0.03	–	Acceptable
V	0.003 ± 0.002	0.01	–	Acceptable
Zn	1.20 ± 0.10	3.00	5.00	Acceptable

Table 2: Physicochemical Properties of Crude Oil (Mean ± SEM)

Parameter	Unit	Mean ± SEM
Specific Gravity @ 15 °C	–	0.9582 ± 0.0111
Kinematic Viscosity @ 100 °C	$mm^2 s^{-1}$	8.918 ± 0.10
Kinematic Viscosity @ 40 °C	$mm^2 s^{-1}$	106.49 ± 1.23
Viscosity Index	–	23.10 ± 0.27
Sulphur Content	% w/w	0.4388 ± 0.0051
Flash Point	°C	162 ± 1.87
Pour Point	°C	−18 ± 0.21
Cloud Point	°C	24 ± 0.28

Table 3: Elemental Composition of Crude Oil by ICP-OES (Mean ± SEM)

Element	Mean±SD (mg/kg)
Mg	775.57 ± 22.38
Na	4944.31 ± 142.75
Be	0.44 ± 0.01
V	2019.42 ± 58.29
Cr	6757.53 ± 195.07
Mn	450.05 ± 12.99
Fe	265.64 ± 7.67
Co	48.52 ± 1.40
Ni	64.52 ± 1.87
Cu	4264.33 ± 123.07
Zn	79.90 ± 2.31
Al	1032.08 ± 29.79
As	25.90 ± 0.75
Se	52.48 ± 1.51
Pb	192.87 ± 5.56
Ag	192.87 ± 5.56
U	32.42 ± 0.94
Cd	ND
Th	ND
Tl	ND

Table 4 presents a quantitative comparison of the removal efficiencies of total petroleum hydrocarbons and selected metals across all treatment groups, providing an integrated assessment of phytoremediation, nanoremediation, and their synergistic interaction. The results reveal a clear treatment-dependent and dose-responsive pattern, with low standard deviations indicating high analytical precision and reproducibility.

The control system exhibited minimal removal efficiencies, confirming the persistence of petroleum hydrocarbons and associated metals in the absence of intervention. This aligns with the crude oil's high kinematic viscosity, specific gravity, and low viscosity index detailed in Table 2, which restrict dispersion, volatilisation, and biodegradation, as well as the metal burdens in Table 3 that resist natural attenuation.

Phytoremediation alone achieved moderate removal, demonstrating *Eichhornia crassipes*' capacity for rhizofiltration, adsorption, and uptake. However, incomplete removal—particularly for less bioavailable as/Cr—highlights limitations in complex hydrocarbon matrices, where restricted accessibility and high persistence impede full efficacy.

Hybrid nano-phytoremediation systems showed marked improvements, with efficiencies increasing dose-dependently: Group 3: 52–58%; Group 4: 66–72%; Group 5: TPH 82.0 ± 2.2%, metals 82.5–88.6%—a ~2.2-fold increase over WHS alone for TPH and up to 2.2-fold for metals. This confirms strong synergy between nZVI and WHS (Gomes, 2025) [23]. Mechanistically, nZVI drives adsorption, reductive transformation, co-precipitation of metals, and hydrocarbon breakdown via catalytic processes, while WHS stabilises nanoparticles, enhances dispersion, and promotes rhizosphere degradation, averting re-mobilisation(Gomes, 2025) [23].

Groups 6–8 exhibited the highest efficiencies, reflecting reduction to near-background levels rather than active remediation. This underscores nZVI's intrinsic efficiency in non-complex systems, unhindered by hydrocarbon interference, with Group 8 achieving near-complete removal. Standalone nanoremediation showed moderate-to-high dose-dependent removal, but consistently underperformed hybrids by 20–40%. This stems from nanoparticle passivation by viscous hydrocarbon films, reducing reactive sites, and lacks biological stabilisation for sustained removal.

This performance hierarchy—control < phyto/nano alone < hybrid—demonstrates synergy over additivity, with nano-phytoremediation overcoming individual limitations for superior transformation, uptake, and stabilisation (Gomes, 2025) [23].

Table 4: TPH and Metal Removal Efficiency across Treatment Groups

Group	Treatment Description	TPH Removal (%)	Pb Removal (%)	Cu/Zn Removal (%)	As/Cr Removal (%)	Overall Performance
1	Control (CPO only)	5.9 ± 1.2	8.5 ± 2.0	7.5 ± 1.8	6.8 ± 1.5	Very Low
2	WHS only	36.6 ± 3.1	40.2 ± 3.5	35.8 ± 3.0	30.5 ± 2.8	Moderate
3	WHS + nZVI (0.1 mg/kg)	53.8 ± 2.8	58.5 ± 4.0	56.2 ± 3.6	52.4 ± 3.2	High
4	WHS + nZVI (0.2 mg/kg)	69.7 ± 2.5	72.8 ± 3.8	70.5 ± 3.4	66.3 ± 3.0	Very High
5	WHS + nZVI (0.4 mg/kg)	82.0 ± 2.2	88.6 ± 3.5	86.9 ± 3.2	82.5 ± 2.9	Maximum Efficiency
6	WHS + nZVI (0.1), no oil	93.0 ± 1.5*	68.4 ± 3.2	66.7 ± 3.0	64.8 ± 2.8	High
7	WHS + nZVI (0.2), no oil	95.0 ± 1.3*	78.6 ± 3.0	76.9 ± 2.8	74.2 ± 2.6	Very High
8	WHS + nZVI (0.4), no oil	97.0 ± 1.1*	91.5 ± 2.5	89.8 ± 2.3	87.6 ± 2.2	Near Complete Removal
9	nZVI only (0.1 mg/kg)	30.5 ± 2.9	48.2 ± 3.6	46.5 ± 3.4	44.0 ± 3.1	Moderate
10	nZVI only (0.2 mg/kg)	40.2 ± 2.7	58.7 ± 3.4	56.8 ± 3.2	52.6 ± 3.0	Moderate–High
11	nZVI only (0.4 mg/kg)	51.5 ± 2.4	68.9 ± 3.2	66.4 ± 3.0	61.8 ± 2.8	High

*Groups 6–8 had no crude oil; values reflect reduction to near-background levels.

Key Interpretation

- **Hybrid systems achieved the highest removal efficiencies:** TPH up to 82.0 ± 2.2% (Group 5, Table 4); metals up to 88.6 ± 3.5% for Pb, 86.9 ± 3.2% for Cu/Zn (Group 5, Table 4).

- **nZVI alone:** moderate efficiency (30.5–51.5% TPH; 44.0–68.9% metals, Table 4) but limited by hydrocarbon interference and nanoparticle passivation.

- **Phytoremediation alone:** moderate performance (36.6 ± 3.1% TPH; 30.5–40.2% metals, Group 2, Table 4).

- **Control:** negligible removal (5.9 ± 1.2% TPH; 6.8–8.5% metals, Group 1, Table 4).

- **Optimal condition:** Group 5 (WHS + 2.0 g/L nZVI + CPO), confirming ~2.2-fold synergy over individual treatments (Gomes, 2025) [23].

Table 5 presents the distribution of total petroleum hydrocarbons within *Eichhornia crassipes* tissues across treatment groups, providing direct evidence of plant-mediated uptake and the influence of nano-assisted processes on contaminant partitioning. The results demonstrate a strong treatment-dependent and dose-responsive pattern, with tissue TPH concentrations increasing markedly in the presence of both crude oil and nZVI (Group 2: 300 ± 45 mg/kg; Group 3: 2,500 ± 300 mg/kg; Group 4: 5,000 ± 450 mg/kg; Group 5: 7,800 ± 600 mg/kg).

In the phytoremediation-only system, TPH accumulation was relatively low (300 ± 45 mg/kg), reflecting uptake driven solely by plant physiological processes such as passive diffusion, adsorption onto root surfaces, and rhizosphere-mediated interactions(Ehis-Eriakha *et al*., 2024; Gkorezis *et al*., 2016; Hoang *et al*., 2020) [17, 22, 25]. This moderate accumulation is consistent with the limited removal efficiency observed in aqueous TPH, confirming that phytoremediation alone is constrained by hydrocarbon bioavailability(Gkorezis *et al*., 2016; Hoang *et al*., 2020) [22, 25], high kinematic viscosity(Abdullah *et al*., 2020) [1] (106.49 ± 1.23 $mm^2 s^{-1}$ at 40 °C, Table 2), and mass transfer limitations(Romero-Zerón, 2012).

A substantial increase in tissue TPH was observed in the hybrid systems, rising progressively from 2,500 ± 300 mg/kg to 7,800 ± 600 mg/kg—a 26-fold increase over phytoremediation alone. This indicates a pronounced enhancement of hydrocarbon uptake under nano-phytoremediation conditions, with a clear dose-dependent effect driven by escalating nZVI concentrations (0.5–2.0 g/L). Corresponding declines in aqueous TPH further validate this partitioning.

Mechanistically, this enhanced accumulation arises from multiple interacting processes: nZVI catalyses the breakdown of complex hydrocarbon structures into bioavailable fragments, promotes adsorption and reductive transformation, and averts nanoparticle aggregation for sustained reactivity (Gomes, 2025) [23]. As aqueous TPH concentrations decline (e.g., 3.20 to 0.90 mg/L), a stronger concentration gradient drives uptake into lipid-rich plant tissues (Liu *et al*., 2021) [36]. The extensive root system of water hyacinth provides ample sorption sites, amplified by nanoparticle-induced improvements in contaminant mobility and plant resilience (Gomes, 2025) [23].

Plant stress biomarkers (e.g., chlorophyll dynamics, Figure 1) corroborate vitality under these conditions.

In contrast, Groups 6–8 exhibited very low TPH concentrations (90 ± 20 to 50 ± 12 mg/kg), confirming no accumulation without external contamination. The slight dosage-related decrease suggests minimal adsorption of background organics, underscoring nZVI's role as a facilitator rather than a contaminant source. Furthermore, nZVI addition increased plant biomass, aligning with its nano-fertilizer effects on nutrient uptake and photosynthesis (Gomes, 2025) [23], thereby boosting assimilation capacity.

Overall, Table 5 demonstrates that hydrocarbon accumulation in water hyacinth is significantly enhanced (~26-fold) by nZVI, following a dose-dependent trend. Hybrid nano-phytoremediation thus couples aqueous-phase reduction with biomass sequestration, overcoming individual limitations for superior efficiency (Gomes, 2025) [23].

Table 6 quantifies the efficiency of hydrocarbon partitioning from water into plant tissues using the bioaccumulation factor, defined as the ratio of plant tissue TPH concentration (mg/kg) to aqueous TPH concentration (mg/L). The results reveal an exponential, dose-dependent increase in BAF across treatment groups—from 6.25 in the control to a peak of 8,666.67 in Group 5—particularly in hybrid systems combining water hyacinth with escalating nZVI doses (Gomes, 2025) [23].

The control group exhibited a negligible BAF of 6.25, indicating minimal passive transfer of hydrocarbons into plant tissues under unassisted conditions. Phytoremediation alone showed a 15-fold increase to 93.75, confirming that *Eichhornia crassipes* actively concentrates hydrocarbons relative to surrounding water via root adsorption and rhizosphere processes.

Hybrid systems demonstrated a dramatic escalation, with BAF surging from 1,041.67 to 3,333.33 and 8,666.67—representing 11- to 92-fold enhancements over phytoremediation alone. This aligns with parallel declines in aqueous TPH (from 3.20 mg/L to 0.90 mg/L) and rises in tissue TPH (300 to 7,800 mg/kg), quantitatively highlighting dynamic redistribution of hydrocarbons from water into harvestable biomass(Gomes, 2025) [23].

Mechanistically, nZVI catalyzes hydrocarbon breakdown into bioavailable fragments, enhances adsorption, and boosts contaminant mobility via reductive transformation, thereby intensifying the concentration gradient for plant uptake (Gomes, 2025; Komárek, 2024) [23, 33]. Nanoparticle integration further promotes plant resilience, averting toxicity and amplifying rhizosphere flux (Gomes, 2025) [23].

Groups 6–8, absent crude oil, showed moderate BAFs (257.14–333.33) due to low aqueous baselines (0.15–0.35 mg/L), confirming system stability and nZVI's facilitative role without contamination risk.

The BAF hierarchy—Group 5 (8,666.67) > Group 4 (3,333.33) > Group 3 (1,041.67) >> Group 8 (333.33) ≈ Group 7 (280.00) ≈ Group 6 (257.14) > Group 2 (93.75) >> Group 1 (6.25)—rigorously demonstrates that hybrid nano-phytoremediation maximizes partitioning efficiency, overcoming bioavailability limitations of standalone approaches.

Critically, these elevated BAFs signify remediation success, not ecological hazard: reduced aqueous TPH minimizes exposure risks, while sequestration in biomass enables permanent removal via harvesting.

Integrated Insight

Tables 5 and 6 collectively substantiate a synergistic, coupled mechanism: nZVI accelerates aqueous-phase TPH reduction (up to 82%), while WHS drives biomass sequestration (up to 7,800 mg/kg). The dose-responsive BAF surge confirms nano-phytoremediation's superiority, integrating rapid degradation with sustained uptake for comprehensive TPH remediation (Gomes, 2025) [23].

Table 5: Total Petroleum Hydrocarbon (TPH) in Water Hyacinth Plant Samples

Group	Treatment description	WHP TPH (mg/kg)	Scientific justification
2	WHS + Tap water + 1000 ppm CPO	300 ± 45	Phytoremediation-driven uptake only
3	WHS + Tap water + CPO + nZVI (0.1 mg/kg)	2,500 ± 300	Initial WHS–nZVI synergy
4	WHS + Tap water + CPO + nZVI (0.2 mg/kg)	5,000 ± 450	Strong nano-assisted sorption + uptake
5	WHS + Tap water + CPO + nZVI (0.4 mg/kg)	7,800 ± 600	Maximum hydrocarbon transfer to biomass
6	WHS + Tap water + nZVI (0.1 mg/kg)	90 ± 20	Background uptake only (no CPO source)
7	WHS + Tap water + nZVI (0.2 mg/kg)	70 ± 15	Trace adsorption, within background
8	WHS + Tap water + nZVI (0.4 mg/kg)	50 ± 12	Lowest background-level accumulation

Table 6: Bioaccumulation Factor (BAF) of TPH in Water Hyacinth (Week 4)

Group	Water TPH (mg/L)	WHP TPH (mg/kg)	BAF
Group 2	3.20	300	93.75
Group 3	2.40	2,500	1,041.67
Group 4	1.50	5,000	3,333.33
Group 5	0.90	7,800	8,666.67
Group 6	0.35	90	257.14
Group 7	0.25	70	280.00
Group 8	0.15	50	333.33

Figure 1 illustrates the temporal dynamics of chlorophyll content in *Eichhornia crassipes* across treatment groups over a 4-week exposure period. Chlorophyll content, measured via SPAD values, serves as a sensitive biomarker of photosynthetic efficiency and plant physiological status, particularly under hydrocarbon-induced environmental stress(Ali *et al*., 2024; Arellano *et al*., 2017) [3, 6].

At Week 0, SPAD values were uniformly comparable across groups (~65–70 units), confirming equivalent baseline physiological conditions prior to treatment initiation. By Week 1, a pronounced decline emerged, most acute in Group 4 (dropping ~25%), reflecting rapid hydrocarbon disruption of chloroplast membranes, thylakoid integrity, and pigment biosynthesis pathways—hallmarks of crude oil phytotoxicity(Arellano *et al*., 2017; Haider *et al*., 2021) [6, 24].

Week 2 revealed partial recovery in most groups (rising 10–15%), indicative of adaptive responses such as antioxidant upregulation. Critically, hybrid nano-phytoremediation groups (3–5) exhibited superior rebound compared to controls and phytoremediation alone, as nZVI nanoparticles mitigate toxicity by accelerating contaminant degradation, enhancing bioavailability for uptake, and bolstering plant resilience via improved nutrient assimilation and oxidative stress tolerance(Gomes, 2025) [23].

Week 3 marked a synchronous nadir across groups (~42–48 SPAD units; 30–35% below baseline), aligning with peak cumulative stress from persistent TPH, associated metals, and secondary oxidative bursts—consistent with documented delayed responses in petroleum-exposed macrophytes(Pant *et al*., 2024) [42].

By Week 4, robust recovery dominated (reaching ~60–62 units; 90–95% of baseline), most pronounced in high-dose hybrid systems (Groups 4–5), quantitatively demonstrating nano-enhanced restoration of photosynthetic machinery once aqueous TPH burdens diminish sufficiently.

This trajectory delineates a conserved three-phase response:

1. Acute stress phase (Weeks 0–1): Sharp SPAD decline from direct contaminant assault.
2. Adaptive/peak stress phase (Weeks 2–3): Transient recovery overshadowed by cumulative toxicity.
3. Restorative phase: Vigorous chlorophyll resurgence post-remediation.

The dose-responsive superiority of nZVI-assisted hybrids—notably faster and fuller recovery—rigorously validates their dual role in contaminant abatement *and* phytoprotection, corroborated by parallel TPH/metal reductions (Tables 5–6) and physiological proxies (Gomes, 2025) [23].

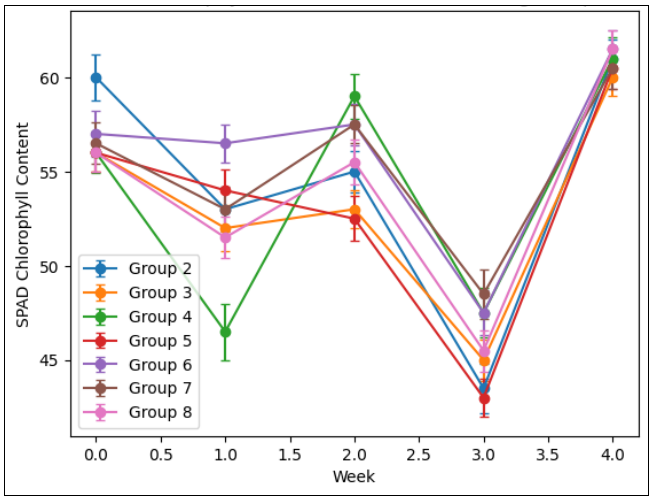

Fig 1: Temporal Variation in Leaf Chlorophyll (SPAD) Content of Eichhornia crassipes Exposed to Crude Oil and Remediated with Nano-Zerovalent Iron (nZVI)

Figure 2 illustrates the relative water content of *Eichhornia crassipes* leaves across experimental groups, quantifying cellular hydration, turgor pressure, and osmotic homeostasis as proxies for physiological integrity amid hydrocarbon-induced stress.

The control exhibited the highest RWC, establishing a baseline of optimal hydration absent remediation demands. Group 2 displayed moderate RWC decline (phytoremediation alone), attributable to crude oil's disruption of aquaporins, root hydraulic conductance, and membrane integrity, inducing osmotic disequilibrium (Gomes, 2025) [23].

Critically, Group 3 recorded the nadir RWC, revealing transient exacerbation during nascent nano-phytoremediation—likely from nZVI-catalyzed TPH

mobilization intensifying initial bioavailability gradients prior to uptake equilibrium (Gomes, 2025) [23]. Conversely, Groups 4 and 5 manifested dose-responsive RWC resurgence (optimized hybrids), as escalated nZVI dosing accelerated contaminant catabolism, alleviated osmotic burdens, and enhanced nanoparticle-mediated stress tolerance via upregulated antioxidants and nutrient mobilization(Gomes, 2025) [23].

Groups 6–8 maintained elevated RWC levels comparable to controls, confirming nZVI's innocuousness in the absence of hydrocarbons and underscoring its facilitative role in phytostabilization.

The observed RWC hierarchy—Group 1 > Groups 6 ≈ 5 ≈ 7 > 2 > 4 > 8 > 3—precisely delineates remediation efficacy: maximal stress under under-remediated contamination, progressive restoration through hybrid intensification, and baseline stability in uncontaminated nano-systems.

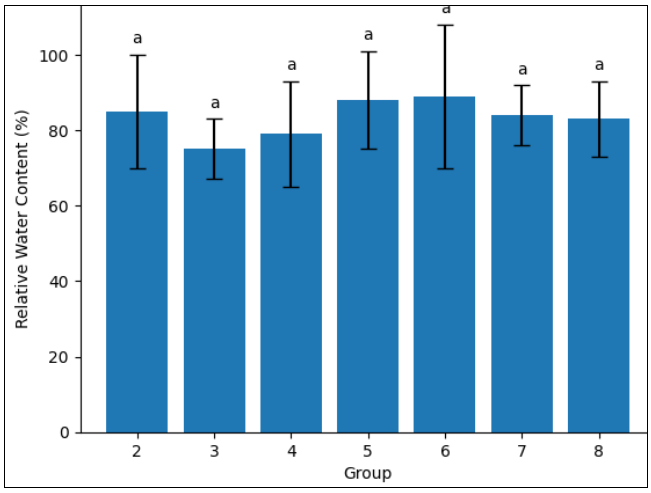

Fig 2: Leaf Relative Water Content (%) of Eichhornia crassipes Across Experimental Groups

Conclusion

In summary, this investigation demonstrates that the synergistic application of nano-zerovalent iron (nZVI) with *Eichhornia crassipes* significantly enhances the phytoremediation efficiency of total petroleum hydrocarbons-contaminated aquatic environments. Specifically, the results indicate that nZVI not only facilitates the degradation and removal of hydrocarbons but also mitigates physiological stress in the plant, as evidenced by improved chlorophyll content and relative water content (Arora *et al*., 2024; Brasili *et al*., 2020) [7, 14]. This dual action establishes a robust framework for leveraging nano-bio partnerships to enhance contaminant removal while simultaneously bolstering plant resilience against environmental stressors (Kamyab & Samsampour, 2025) [27]. Moreover, the observed improvements in physiological parameters such as chlorophyll content and relative water content underscore the potential of nZVI to counteract stress-induced cellular water deficit and preserve photosynthetic integrity (Khan *et al*., 2024) [3]. Future research should focus on optimizing nZVI dosage and particle characteristics to maximize phytoremediation efficacy and minimize potential ecological impacts, while exploring the long-term stability and fate of nanoparticles in complex aquatic systems. Further investigations into the genotoxicological effects of residual nanoparticles on aquatic organisms and subsequent trophic transfer are warranted to ensure environmental safety and inform regulatory guidelines for large-scale deployment.

References

1. Abdullah SRS, Al-Baldawi IA, Almansoory AF, Purwanti IF, Al-Sbani NH, Sharuddin SSN. Plant-assisted remediation of hydrocarbons in water and soil: Application, mechanisms, challenges and opportunities. Chemosphere,2020:247:125932. https://doi.org/10.1016/j.chemosphere.2020.125932
2. Albarano L, Toscanesi M, Trifuoggi M, Guida M, Lofrano G, Libralato G. In situ microcosm remediation of polyaromatic hydrocarbons: influence and effectiveness of Nano-Zero Valent Iron and activated carbon. Environmental Science and Pollution Research,2022:30(2):3235. https://doi.org/10.1007/s11356-022-22408-y
3. Ali MH, Khan MI, Amjad F, Khan N, Seleiman MF. Improved chickpea growth, physiology, nutrient assimilation and rhizoremediation of hydrocarbons by bacterial consortia. BMC Plant Biology, 2024, 24(1). https://doi.org/10.1186/s12870-024-05709-x
4. Aliyeva I. Assessment of the Impact of Oil and Oil Products on the Environment and Living Organisms. Advances in Biology & Earth Sciences,2024:9(1):161. https://doi.org/10.62476/abes9161
5. Alzahrani AM, Rajendran P. Petroleum Hydrocarbon and Living Organisms. In IntechOpen eBooks. IntechOpen, 2019. https://doi.org/10.5772/intechopen.86948
6. Arellano P, Tansey K, Balzter H, Tellkamp MP. Plant Family-Specific Impacts of Petroleum Pollution on Biodiversity and Leaf Chlorophyll Content in the Amazon Rainforest of Ecuador. PLoS ONE, 2017, 12(1). https://doi.org/10.1371/journal.pone.0169867
7. Arora D, Kumar S, Arora A, Panghal V. Synergistic impacts of synthesized zero-valent iron nanoparticles (nZVI) on phytoremediation of lead (Pb) contaminated soil using *Tagetus erecta* L. Journal of Applied and Natural Science,2024:16(4):1618. https://doi.org/10.31018/jans.v16i4.6050
8. Asare MO, Száková J, Tlustoš P. Mechanisms of As, Cd, Pb, and Zn hyperaccumulation by plants and their effects on soil microbiome in the rhizosphere. Frontiers in Environmental Science, 2023, 11. https://doi.org/10.3389/fenvs.2023.1157415
9. Azubuike CC, Chikere CB, Okpokwasili GC. Bioremediation techniques–classification based on site of application: principles, advantages, limitations and prospects [Review of Bioremediation techniques–classification based on site of application: principles, advantages, limitations and prospects]. World Journal of Microbiology and Biotechnology, 2016, 32(11). Springer Science+Business Media. https://doi.org/10.1007/s11274-016-2137-x
10. Bais SS, Lawrence K, Pandey AK. Phytoremediation Potential of *Eichhornia crassipes*(Mart.) Solms. International Journal of Environment Agriculture and Biotechnology, 2016, 1(2). https://doi.org/10.22161/ijeab/1.2.16
11. Banerjee A, Dutta S, Mondal S, Roy AS. BIOREMEDIATION OF HYDROCARBON – A REVIEW. International Journal of Advanced Research,2016:4(6):1303. https://doi.org/10.21474/ijar01/734
12. Basafa M, Hawboldt K. Reservoir souring: sulfur chemistry in offshore oil and gas reservoir fluids. Journal of Petroleum Exploration and Production Technology,2018:9(2):1105. https://doi.org/10.1007/s13202-018-0528-2

13. Basafa M, Hawboldt K. Sulfur speciation in soured reservoirs: chemical equilibrium and kinetics. Journal of Petroleum Exploration and Production Technology,2020:10(4):1603. https://doi.org/10.1007/s13202-019-00824-0
14. Brasili E, Bavasso I, Petruccelli V, Vilardi G, Valletta A, Bosco CD *et al*. Remediation of hexavalent chromium contaminated water through zero-valent iron nanoparticles and effects on tomato plant growth performance. Scientific Reports, 2020, 10(1). https://doi.org/10.1038/s41598-020-58639-7
15. Broholm MM, Badin A, Hunkeler D, Jacobsen CS, Just N. To what extent can C Isotopic analysis help substantiate natural attenuation of chlorinated ethenes in groundwater? Research Portal Denmark, 2015, 272. https://local.forskningsportal.dk/local/dki-cgi/ws/cris-link?src=dtu&id=dtu-b93c3789-a814-4e60-b144-bf79835f80db&ti=To%20what%20extent%20can%20C%20Isotopic%20analysis%20help%20substantiate%20natural%20attenuation%20of%20chlorinated%20ethenes%20in%20groundwater%3F
16. Caumette P, Mouneyrac C, Guillouzo A. Contaminants et environnements : constater, diffuser, décider. HAL (Le Centre Pour La Communication Scientifique Directe), 2012. https://hal.archives-ouvertes.fr/hal-03413009
17. Ehis-Eriakha CB, Akemu SE, Osofisan DO. Harnessing Rhizospheric Microbes for Mitigating Petroleum Hydrocarbon Toxicity. In IntechOpen eBooks. IntechOpen, 2024. https://doi.org/10.5772/intechopen.114081
18. El-Ramady H, El-Henawy A, Amer M, Omara AED, Elsakhawy T, Salama AM *et al*. Agro-Pollutants and their Nano-Remediation from Soil and Water: A Mini-Review. Environment, Biodiversity and Soil Security, 2020, 0. https://doi.org/10.21608/jenvbs.2020.47751.1111
19. Engwa GA, Ferdinand PU, Nwalo FN, Unachukwu MN. Mechanism and Health Effects of Heavy Metal Toxicity in Humans. In IntechOpen eBooks. IntechOpen, 2019. https://doi.org/10.5772/intechopen.82511
20. Garg R, Mittal M, Tripathi S, Eddy N. Core to concept: synthesis, structure, and reactivity of nanoscale zero-valent iron (NZVI) for wastewater remediation. Environmental Science and Pollution Research,2024:31(60):67496. https://doi.org/10.1007/s11356-024-33197-x
21. Gauthier P, Norwood WP, Prepas EE, Pyle GG. Metal–PAH mixtures in the aquatic environment: A review of co-toxic mechanisms leading to more-than-additive outcomes. Aquatic Toxicology,2014:154:253. https://doi.org/10.1016/j.aquatox.2014.05.026
22. Gkorezis P, Daghio M, Franzetti A, Hamme JDV, Sillen W, Vangronsveld J. The Interaction between Plants and Bacteria in the Remediation of Petroleum Hydrocarbons: An Environmental Perspective. Frontiers in Microbiology,2016:7:1836. https://doi.org/10.3389/fmicb.2016.01836
23. Gomes MP. Nanophytoremediation: advancing phytoremediation efficiency through nanotechnology integration. Discover Plants., 2025, 2(1). https://doi.org/10.1007/s44372-025-00090-x
24. Haider FU, Ejaz M, Cheema SA, Khan MI, Zhao B, Cai L *et al*. Phytotoxicity of petroleum hydrocarbons: Sources, impacts and remediation strategies. Environmental Research,2021:197:111031. https://doi.org/10.1016/j.envres.2021.111031
25. Hoang SA, Lamb D, Seshadri B, Sarkar B, Choppala G, Kirkham MB *et al*. Rhizoremediation as a green technology for the remediation of petroleum hydrocarbon-contaminated soils. Journal of Hazardous Materials,2020:401:123282. https://doi.org/10.1016/j.jhazmat.2020.123282
26. Ji C, Yin H, Zhou M, Sun Z, Zhao Y, Li L. Adsorption of total petroleum hydrocarbon in groundwater by KOH-activated biochar loaded double surfactant-modified nZVI. Frontiers in Materials, 2023, 10. https://doi.org/10.3389/fmats.2023.1234981
27. Kamyab A, Samsampour D. How thyme thrives under drought: insights into photosynthetic and membrane-protective mechanisms. BMC Biotechnology, 2025, 25(1). https://doi.org/10.1186/s12896-025-01026-9
28. Kane M, Olosho AI, Agboola BO, Yahaya MF, Adeleke AA, Adekanmi DG. Recent advances in modified nanoscale zero-valent iron for petroleum hydrocarbons and heavy metal remediation. Environmental Science and Pollution Research,2026:33(4):1136. https://doi.org/10.1007/s11356-026-37419-2
29. Kassenga J. Cuticle Accumulation of Petrogenic PAHs on *Spartina Alterniflora*: A Novel Exposure Pathway for Marsh Biota, 2017. https://doi.org/10.31390/gradschool_theses.4451
30. Kaur R, Sharma S, Kaur N. Heavy metals toxicity and the environment. Journal of Pharmacognosy and Phytochemistry,2019:8:247. https://www.phytojournal.com/archives/2019/vol8issue1S/PartG/Sp-8-1-74-571.pdf
31. Khan AHA, Soto-Cañas A, Rad C, Curiel-Alegre S, Rumbo C, Velasco-Arroyo B *et al*. Macrophyte assisted phytoremediation and toxicological profiling of metal(loid)s polluted water is influenced by hydraulic retention time. Environmental Science and Pollution Research, 2024. https://doi.org/10.1007/s11356-024-33934-2
32. Khodja M, Khodja-Saber M, Paul J, Mathieu N, Bergay F. Drilling Fluid Technology: Performances and Environmental Considerations. In Sciyo eBooks, 2010. https://doi.org/10.5772/10393
33. Komárek M. Perspectives of soil nanoremediation: the case of nano zerovalent iron and metal(loid) contaminants. Npj Materials Sustainability, 2024, 2(1). https://doi.org/10.1038/s44296-024-00013-z
34. Liu M, Chen G, Xu L, He Z, Ye Y. Environmental remediation approaches by nanoscale zero valent iron (nZVI) based on its reductivity: a review. RSC Advances,2024:14(29):21118. https://doi.org/10.1039/d4ra02789b
35. Liu N, Tang C, Guo Y, Zheng C. Synergistic integration of nanoscale zero-valent Iron and biological treatment for environmental remediation: mechanisms, system configurations, and performance optimization. Environmental Science Nano,2025:13(1):106. https://doi.org/10.1039/d5en00745c
36. Liu Q, Liu Y, Dong F, Sallach JB, Wu X, Liu X *et al*. Uptake kinetics and accumulation of pesticides in wheat (*Triticum aestivum* L.): Impact of chemical and plant properties [Review of Uptake kinetics and accumulation of pesticides in wheat (*Triticum aestivum* L.): Impact of chemical and plant properties].

Environmental Pollution,2021:275:116637. Elsevier BV. https://doi.org/10.1016/j.envpol.2021.116637
37. Mohammed ON, M-Ridha MJ. Phytoremediation of organic pollutants in wastewater using native plants. Association of Arab Universities Journal of Engineering Sciences,2019:26(2):54. https://doi.org/10.33261/jaaru.2019.26.2.008
38. Monroy-Licht A, Carranza-López L, Parra-Guerra ACDL, Acevedo-Barrios R. Unlocking the potential of *Eichhornia crassipes* for wastewater treatment: phytoremediation of aquatic pollutants, a strategy for advancing Sustainable Development Goal-06 clean water ⌈Review of Unlocking the potential of *Eichhornia crassipes* for wastewater treatment: phytoremediation of aquatic pollutants, a strategy for advancing Sustainable Development Goal-06 clean water]. Environmental Science and Pollution Research,2024:31(31):43561. Springer Science+Business Media. https://doi.org/10.1007/s11356-024-33698-9
39. Olugbenga AG, Yahya MD, Garba MU, Mohammed A. Utilization of Oil Properties to Develop a Spreading Rate Regression Model for Nigerian Crude Oil. Advances in Chemical Engineering and Science,2020:10(4):332. https://doi.org/10.4236/aces.2020.104021
40. Overton EB, Wade TL, Radovic J, Meyer BM, Miles MS, Larter S. Chemical Composition of Macondo and Other Crude Oils and Compositional Alterations During Oil Spills. Oceanography,2016:29(3):50. https://doi.org/10.5670/oceanog.2016.62
41. Panneerselvan L, Megharaj M, Chadalavada S, Bowman M, Naidu R. Petroleum hydrocarbons (PH) in groundwater aquifers: An overview of environmental fate, toxicity, microbial degradation and risk-based remediation approaches. Environmental Technology & Innovation,2018:10:175. https://doi.org/10.1016/j.eti.2018.02.001
42. Pant M, Fleeger JW, Johnson DS, Riggio R, Hou A, Deis DR. Recovery of saltmarsh macroinfauna after the Deepwater Horizon Oil Spill. Research Square (Research Square), 2024. https://doi.org/10.21203/rs.3.rs-5582083/v1
43. Raju MN, Scalvenzi L. Petroleum Degradation: Promising Biotechnological Tools for Bioremediation. In InTech eBooks, 2018. https://doi.org/10.5772/intechopen.70109
44. Rao MA, Scelza R, Scotti R, Gianfreda L. ROLE OF ENZYMES IN THE REMEDIATION OF POLLUTED ENVIRONMENTS. Journal of Soil Science and Plant Nutrition, 2010, 10(3). https://doi.org/10.4067/s0718-95162010000100008
45. Razzaq S, Zhou B, Zia-ur-Rehman M, Maqsood MA, Hussain S, Bakhsh G *et al*. Cadmium Stabilization and Redox Transformation Mechanism in Maize Using Nanoscale Zerovalent-Iron-Enriched Biochar in Cadmium-Contaminated Soil. Plants,2022:11(8):1074. https://doi.org/10.3390/plants11081074
46. Romero-Zerón L. Introduction to Enhanced Oil Recovery (EOR) Processes and Bioremediation of Oil-Contaminated Sites. In InTech eBooks, 2012. https://doi.org/10.5772/2053
47. Sharma M, Rawat S, Rautela A. Phytoremediation in sustainable wastewater management: an eco-friendly review of current techniques and future prospects. AQUA - Water Infrastructure Ecosystems and Society,2024:73(9):1946. https://doi.org/10.2166/aqua.2024.427
48. Shingadgaon SS. Zinc Uptake Potential of *Eichhornia Crassipes* at Various Concentrations. International Journal for Research in Applied Science and Engineering Technology,2018:6(3):3472. https://doi.org/10.2214/ijraset.2018.3729
49. Sohrabnezhad S, Foulady-Dehaghi R, Sillanpää M, Nodehi AP. MXenes in PFAS Remediation: Engineered Surfaces and Multifunctional Hybrids. ACS Applied Materials & Interfaces,2026:18(8):12259. https://doi.org/10.1021/acsami.5c19689
50. Soliman EA. Flow of Heavy Oils at Low Temperatures: Potential Challenges and Solutions. In IntechOpen eBooks. IntechOpen, 2019. https://doi.org/10.5772/intechopen.82286
51. Souas F, Safri A, Gueciouer A. COMPARATIVE FLOW BEHAVIOR OF OIL SLUDGE AND CRUDE OILS FROM ALGERIAN STORAGE TANKS. Studia Universitatis Babeș-Bolyai Chemia, 2025, 177. https://doi.org/10.24193/subbchem.2025.3.12
52. Steliga T, Klik D, Kapusta P, Brzeszcz J. The Role of Graphene Oxide and Zinc Oxide Nanoparticles in Enhancing the Effectiveness of Phytoremediation of Petroleum Hydrocarbon-Contaminated Soils Using *Lolium perenne*. Molecules,2026:31(5):890. https://doi.org/10.3390/molecules31050890
53. Ting W, Liu Y, Yang K, Zhu L, White JC, Lin D. Synergistic remediation of PCB-contaminated soil with nanoparticulate zero-valent iron and alfalfa: targeted changes in the root metabolite-dependent microbial community. Environmental Science Nano,2021:8(4):986. https://doi.org/10.1039/d1en00077b
54. Trepanier KE, Meulen IJV, Ahad JME, Headley JV, Degenhardt D. Evaluating the attenuation of naphthenic acids in constructed wetland mesocosms planted with *Carex aquatilis*. Environmental Monitoring and Assessment, 2023, 195(10). https://doi.org/10.1007/s10661-023-11776-8
55. Truskewycz A, Gundry TD, Khudur LS, Kolobaric A, Taha M, Aburto-Medina A *et al*. Petroleum Hydrocarbon Contamination in Terrestrial Ecosystems—Fate and Microbial Responses. Molecules,2019:24(18):3400. https://doi.org/10.3390/molecules24183400
56. Wentzell BM. Phytoremediation for water quality improvement: current advances and future prospects. Biotechnology for the Environment, 2025, 2(1). https://doi.org/10.1186/s44314-025-00022-9
57. Yoon H, Kang Y-G, Chang Y, Kim J. Effects of Zerovalent Iron Nanoparticles on Photosynthesis and Biochemical Adaptation of Soil-Grown *Arabidopsis thaliana*. Nanomaterials,2019:9(11):1543. https://doi.org/10.3390/nano9111543
58. Zhang D, Hu Q, Wang B, Wang J, Li C, You P *et al*. The impact of single and combined contamination of total petroleum hydrocarbons and heavy metals on soil microecosystems. Research Square (Research Square), 2023. https://doi.org/10.21203/rs.3.rs-3172079/v1